

QUENCHING OF THE QUIESCENT H-PHASE IN ASDEX

E.R. Müller, G. Fussmann, G. Janeschitz, H.D. Murmann, A. Stäbler
and the ASDEX- and NI-Teams

Max-Planck-Institut für Plasmaphysik
EURATOM Association, D-8046 Garching, Fed. Rep. of Germany

Introduction

Highest energy confinement during neutral-beam heating is obtained when the discharge is in the quiescent, ELM-free H-mode. The improved energy confinement is linked to higher particle and also impurity confinement / 1 /. In the original ASDEX DV-I divertor configuration and with stainless-steel vessel walls, this resulted in an accumulation of metallic impurities. The excessive radiation power losses terminated the H-phase after about 100 ms / 2 /. After carbonization of the walls aimed at reducing the metallic impurity content and, secondly, the prolongation of the ASDEX NI-heating pulse in the new DV-II divertor configuration / 3 /, much longer quiescent H-phases could be expected. This, however, was not achieved. After a quiescent phase of less than 150 ms, the H-mode converts back into the L-mode.

Plasma parameter evolution

Fig. 1 shows the time evolution of various plasma parameters during discharge # 24939 which exhibits an ELM-free H-phase from 1.19 to 1.325 s ($I_p = 380$ kA, $B_t = 2.36$ T, $\bar{n}_e(0.95 \text{ s}) = 3.7 \times 10^{13} \text{ cm}^{-3}$, $P_{NI} = 1.3$ MW, $D^0 \rightarrow D^+$ co-injection, DV-II divertor configuration in single-null operation, slightly carbonized walls). The L-phase between 1.0 and 1.19 s does not become fully stationary (see gas feed rate). There are three characteristic times during the H-phase: Firstly, the L- to H-mode transition at 1.19 s, indicated by the sharp drop in the D_α -signal, is triggered by a sawtooth (see soft X-ray intensity). The improved energy and particle confinement result in rising β_p and \bar{n}_e (the gas valve switches off). Global radiation power losses (P_{RAD}) and local radiation power losses at the plasma centre ($P_{RAD}(0)$) start to grow as well. This is only partly due to the density rise but also due to impurity accumulation, as is demonstrated by the increasing $Z_{eff}(0)$ value at the plasma centre ($Z_{eff}(a/2)$ decreases / 4 /). The time evolution of $P_{RAD}(0)$ is closely correlated with that of soft X-ray and metallic impurity line intensities, which are emitted from the plasma core. The OVI line intensity, more representative of the impurity influx at the plasma edge, is fairly constant. At 1.27 s, the second characteristic time, β_p saturates at a value of 1.2. While density and radiation losses continue to grow, $T_{e,0}$ and $Z_{eff}(0)$ begin to decline. In contrast, $T_e(a/2)$ (see Fig. 2) and $Z_{eff}(a/2)$ go up. Sawteeth are visible on the soft X-ray signal over the entire H-phase. At 1.325 s, the third time mark, the H-mode is terminated by sudden collapse producing simultaneous dips or peaks on most centre and edge signals. While the discharge falls back into the L-mode, it develops transiently its highest $P_{RAD}(0)$ and $Z_{eff}(0)$ values. At about 1.70 s, a really stationary L-mode is reached with much lower values of $T_{e,0}$ and β_p and much higher ones of $P_{RAD}(0)$ and loop voltage (U_L) than during the first L-mode at 1.15 s.

As usual, in the H-mode the n_e profiles are broader and the T_e profiles are higher at the edge than in the L-mode (Fig. 2). But, with the more open DV-II divertor configuration / 3 /, the n_e profiles of the H-mode are even flatter in the centre and steeper at the edge than those obtained with the more closed DV-I configuration.

Impurity accumulation at the plasma centre

Fig. 3 shows the central peaking of the P_{RAD} profile during the quiescent H-mode, which is only partly caused by the increase of the n_e and the decrease of the T_e profiles (Fig. 2), but which mainly reflects the accumulation of metallic impurities with medium-Z value at the plasma centre (accumulation of low-Z elements cannot be excluded). Copper originates from the new divertor target plates, iron from the weakly carbonized walls. Accumulation has been simulated quantitatively using the model described in Ref. /5/: The influx of metals ($\Phi_{\text{Cu}} = 1.5 \times 10^{19} \text{ s}^{-1}$) does not change at the L- to H-mode conversion. But the anomalous diffusion coefficient drops by an order of magnitude ($D_{\text{an}} = 0.9 \rightarrow 0.1 \text{ m}^2/\text{s}$) over the whole plasma cross-section, thus suppressing the impurity outward flow. Since neoclassical inward drift ($v_{\text{Fe}}(a/2) = 0.8 \text{ m/s}$) is not counteracted any more, this leads to impurity accumulation. At the β_p maximum (1.27 s), metal concentrations of 0.5 % are attained at the plasma centre, with equal contributions of iron and copper.

The extremely high central radiation values ($P_{\text{RAD}}(0)$ in Fig. 3) can be sustained stationary during the second L-phase (1.70 s) in association with lower $T_e(r)$ (Fig. 2). In contrast to the first L-phase at 1.15 s, the second L-phase is sawteeth-free.

Quenching of the quiescent H-mode by central radiation losses

Fig. 4 presents the time variation of the global power balance and Fig. 5 of the local one for the plasma centre. Neutral-beam power depositions have been calculated with the FREYA code. The power deposition onto the divertor target plates was not measured, which may explain the missing power in some global balances. The blocking of the energy flow into the divertor during the quiescent H-mode /6/ is less perfect with the present DV-II divertor (see RAD_{div}) than the former DV-I. Radiation power losses volume-integrated over the outer plasma half-radius (RAD_{edge}) always dominate over radiation losses from the inner half-radius ($\text{RAD}_{\text{center}}$). But, it is mainly the enhancement of $\text{RAD}_{\text{center}}$ by a factor of 5 that raises the global radiation power losses, $\text{RAD}_{\text{center}} + \text{RAD}_{\text{edge}}$, from 46% of the total heating power in the ohmic and L-phase(s) to 82 % at the collapse of the H-mode. For compensation of such high radiation losses and the power losses into the divertor, energy is taken from the plasma ($dW/dt < 0$).

The local power balance at the plasma centre reveals, that the quiescent H-mode is quenched when the central radiation power losses $P_{\text{RAD}}(0)$ reach $1 \text{ W}\cdot\text{cm}^{-3}$ which is almost exactly hundred per cent of the local heating power ($P_{\text{OH}}(0) + P_{\text{NI}}(0)$). Power for transport losses must be drawn from the energy reservoir of the plasma ($dW(0)/dt < 0$).

Conclusion

During the ELM-free H-mode, impurity accumulation in the plasma core occurs as a consequence of improved confinement. The exponentially growing radiation power losses at the plasma centre become as high as the local power input and, thus, quench the H-mode. The β_p saturation (1.27 s) cannot be attributed to radiation power losses from the plasma centre ($r < 20 \text{ cm}$); perhaps, radiation losses at outer radii play a role.

References

- /1/ M. Keilhacker, et al., 10th Int. Conf. London 1984, IAEA 1 (1985) 71.
- /2/ E.R. Müller, et al., Nucl. Fus. 27 (1987) 1817.
- /3/ H. Niedermeyer, et al., Pl. Phys. and Contr. Fusion 30 (1988) 1443.
- /4/ K.H. Steuer, et al., this conference.
- /5/ G. Fußmann, et al., 8th PSI conference, to be published in Journ. Nucl. Mat.
- /6/ E.R. Müller, et al., Journ. Nucl. Mat. 121 (1984) 138.

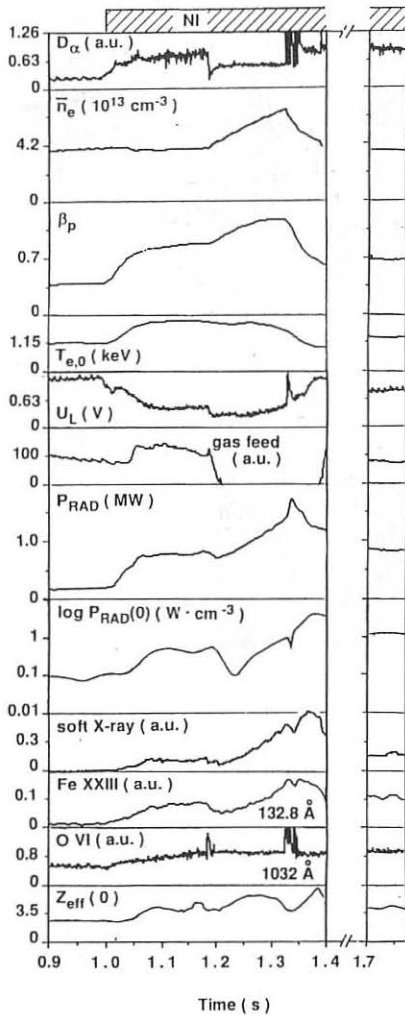


Fig. 1 : Time evolution of various plasma parameters during discharge # 24939 which shows an ELM-free H phase. ($I_p = 380$ kA, $B_1 = 2.36$ T, $P_{NI} = 1.3$ MW, $D^0 \rightarrow D^+$, DV-II divertor configuration in single-null operation ($\Delta z = 2$ cm), carbonized walls)

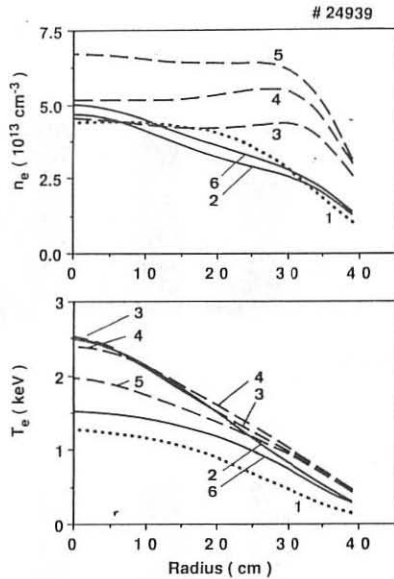


Fig. 2 : Radial profiles of electron density n_e and temperature T_e at typical times during discharge # 24939 (the L or H mode character is indicated behind the time value).
 (1) $t = 0.950$ s (L) (4) $t = 1.270$ s (H)
 (2) $t = 1.150$ s (L) (5) $t = 1.325$ s (H)
 (3) $t = 1.210$ s (H) (6) $t = 1.700$ s (L)

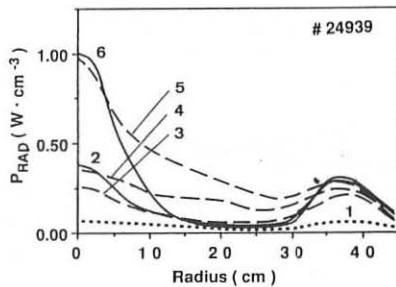


Fig. 3 : Bolometrically determined radial profiles of radiation power density (at same times as in Fig. 2).

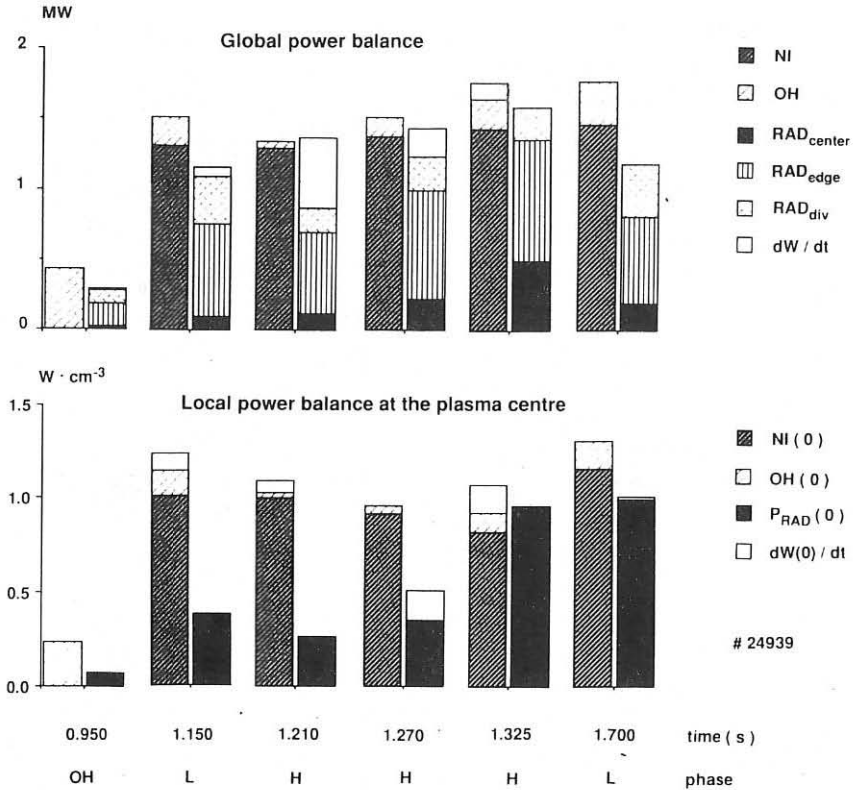


Fig. 4 (above) :
Time evolution of the global power balance of discharge # 24939 :

Power input channels : the neutral-injection heating power (NI) and the Ohmic heating power (OH) .

Power loss channels : bolometrically determined radiation and neutral particle power losses, volume-integrated over the inner plasma half-radius (RAD_{center}) and over the outer half-radius (RAD_{edge}), and the volume power losses of the plasma within the divertor chambers (RAD_{div}), determined by bolometers as well.

Fig. 5 (below) :
Time evolution of the local power balance at the plasma centre of discharge # 24939 :

P_{RAD}(0) denotes the bolometrically determined local radiation power losses at the plasma centre, and NI(0), OH(0), dW(0)/dt represent also local values.

Dependig on their sign, the time derivatives of the respective plasma energy contents, dW/dt and dW(0)/dt, are added to the input or loss channels.